

Have hierarchical three-body mergers been detected by LIGO/Virgo?

Doğa Veske,¹★ Zsuzsa Márka,² Andrew G. Sullivan,¹ Imre Bartos,³
K. Rainer Corley,^{1,2} Johan Samsing⁴ and Szabolcs Márka¹

¹*Department of Physics, Columbia University in the City of New York, 550 W 120th St., New York, NY 10027, USA*

²*Columbia Astrophysics Laboratory, Columbia University in the City of New York, 550 W 120th St., New York, NY 10027, USA*

³*Department of Physics, University of Florida, PO Box 118440, Gainesville, FL 32611-8440, USA*

⁴*Niels Bohr International Academy, The Niels Bohr Institute, Blegdamsvej 17, DK-2100, Copenhagen, Denmark*

31 July 2020

ABSTRACT

One of the proposed channels of binary black hole mergers involves dynamical interactions of three black holes. In such scenarios, it is possible that all three black holes merge in a so-called hierarchical merger chain, where two of the black holes merge first and then their remnant subsequently merges with the remaining single black hole. Depending on the dynamical environment, it is possible that both mergers will appear within the observable time window. Here we perform a search for such merger pairs in the public available LIGO and Virgo data from the O1/O2 runs. Using a frequentist p-value assignment statistics we do not find any significant merger pair candidates, the most significant being GW170809-GW151012 pair. Assuming no observed candidates in O3/O4, we derive upper limits on merger pairs to be $\sim 11 - 110 \text{ year}^{-1} \text{Gpc}^{-3}$, corresponding to a rate that relative to the total merger rate is $\sim 0.1 - 1.0$. From this we argue that both a detection and a non-detection within the next few years can be used to put useful constraints on some dynamical progenitor models.

Key words: gravitational waves – (transients:) black hole mergers

1 INTRODUCTION

The LIGO Scientific Collaboration and the Virgo Collaboration have publicly announced properties of 10 binary black hole (BBH) mergers from the first and second observing runs (O1 and O2) in the gravitational wave (GW) catalog GWTC-1 (Abbott et al. 2019a). Individual groups have also performed searches on the open data from O1 and O2 and found additional merger candidates (Venumadhav et al. 2020; Zackay et al. 2019a; Nitz et al. 2019; Zackay et al. 2019b). From those, Venumadhav et al. (2020); Zackay et al. (2019a,b) report 8 more BBH mergers, total of 18 BBH mergers, whose samples are publicly available at https://github.com/jroulet/O2_samples (IAS-Princeton mergers hereafter). The set of confirmed events have been used to constrain e.g. general relativity and its possible modifications (e.g. LIGO Scientific Collaboration et al. 2019); however, how and where the BBHs form in our Universe are still major unsolved questions. There are several plausible formation scenarios, including field binaries (Dominik et al. 2012, 2013, 2015; Belczynski et al. 2016b,a; Silsbee & Tremaine 2017; Murguía-Berthier et al. 2017; Rodriguez & Antonini 2018; Schröder et al. 2018), chemically homogeneous binary evolution (De Mink & Mandel 2016; Mandel & de Mink

2016; Marchant, Pablo et al. 2016), dense stellar clusters (Portegies Zwart & McMillan 2000; Banerjee et al. 2010; Tanikawa 2013; Bae et al. 2014; Rodriguez et al. 2015, 2016a,b; Askar et al. 2017; Park et al. 2017), active galactic nuclei (AGN) discs (Bartos et al. 2017b; Stone et al. 2017; McKernan et al. 2018; Yang et al. 2019b), galactic nuclei (GN) (O’Leary et al. 2009; Hong & Lee 2015; VanLandingham et al. 2016; Antonini & Rasio 2016; Stephan et al. 2016; Hoang et al. 2018; Hamers et al. 2018), very massive stellar mergers (Loeb 2016; Woosley 2016; Janiuk et al. 2017; D’Orazio & Loeb 2018), and single-single GW captures of primordial black holes (Bird et al. 2016; Cholis et al. 2016; Sasaki et al. 2016; Carr et al. 2016). The question is; how do we observationally distinguish these merger channels from each other? Recent work has shown that the measured BH spin (Rodriguez et al. 2016c), mass spectrum (Zevin et al. 2017; Yang et al. 2019a), and orbital eccentricity (Samsing et al. 2014; Samsing & Ramirez-Ruiz 2017; Samsing et al. 2018a; Samsing 2018; Samsing et al. 2018b; Samsing & D’Orazio 2018; Zevin et al. 2019; Rodriguez et al. 2018b; Samsing et al. 2020; Samsing et al. 2019b) can be used. In addition, indirect probes of BH populations have also been suggested; for example, stellar tidal disruption events can shed light on the BBH orbital distribution and corresponding merger rate in dense clusters (e.g. Samsing et al. 2019a), or spatial correlations with host galaxies (Bartos et al. 2017a).

★ E-mail: dv2397@columbia.edu

In this paper we perform the first search for a feature we denote

‘hierarchical merger chains’ that are unique to highly dynamical environments (e.g. [Samsing & Ilan 2018a](#); [Samsing & Ilan 2018b](#)). The most likely scenario of a hierarchical merger chain is the interaction of three BHs, $\{BH_1, BH_2, BH_3\}$, that undergo two subsequent mergers; the first between $\{BH_1, BH_2\}$ and the second between $\{BH_{12}, BH_3\}$, where BH_{12} is the BH formed in the first merger. Such hierarchical merger chains have been shown to form in e.g. globular clusters (GCs) as a result of binary-single interactions. In this case, the first merger happens during the three-body interaction when the BHs are still bound to each other, which makes it possible for the merger remnant to subsequently merge with the remaining single BH ([Samsing & Ilan 2018a](#); [Samsing & Ilan 2018b](#)). Fig. 1 illustrates schematically this scenario. Such few-body interactions are not restricted to GCs, but can also happen in e.g. AGN discs (e.g. [Tagawa et al. 2019](#)). Interestingly, under certain orbital configurations, both the first and the second merger can show up as detectable GW signals within the observational time window (e.g. [Samsing & Ilan 2018b](#)). The hierarchical merger chain scenario can therefore be observationally constrained, and can as a result be used to directly probe the dynamics leading to the assembly of GW sources.

With this motivation, we here look for hierarchical merger pair events in the public O1 and O2 data from LIGO and Virgo. For this, we present a new algorithm to identify merger pairs, the simplest example of a hierarchical merger chain, and use it to search for such events in the public GWTC-1 catalogue and in the IAS-Princeton sample.

The paper is organized as follows. In Section 2 we describe our search method, and in Section 3 we present the corresponding results. Finally, we conclude our work in Section 4.

2 SEARCH

In this section we describe our methods for searching for GW merger pairs originating from three-body interactions like the one shown in Fig. 1.

2.1 Parameters

Our search is based on a frequentist p-value assignment by using a test statistic (TS). As Neyman-Pearson’s lemma suggests ([Neyman et al. 1933](#)), we choose our TS to be the ratio of the likelihood of the signal hypothesis to the likelihood of the null hypothesis; where we define our null hypothesis H_0 as having two unrelated mergers, and our signal hypothesis H_s as having two related mergers originating from a three-body interaction. We use 3 parameters of the BBH mergers for calculating the likelihood ratio:

- *Mass estimates*: One of the initial BH masses in the second merger should agree with the final mass of the BH formed in the first merger.
- *Correct time order*: The first merger, as defined by the mass difference, should happen before the second merger.
- *Localization*: Both the first and the second merger must originate from the same spatial location.

Using these three parameters our TS is

$$TS = \begin{cases} \frac{\mathcal{L}(M_f, m_{1,s}, m_{2,s}, V_f, V_s | H_s)}{\mathcal{L}(M_f, m_{1,s}, m_{2,s}, V_f, V_s | H_0)} & , t_f < t_s \\ 0 & , t_f \geq t_s \end{cases} \quad (1)$$

where \mathcal{L} represents the likelihoods of the parameters for each hypothesis, M represents the final mass estimate, m_1 and m_2 represent

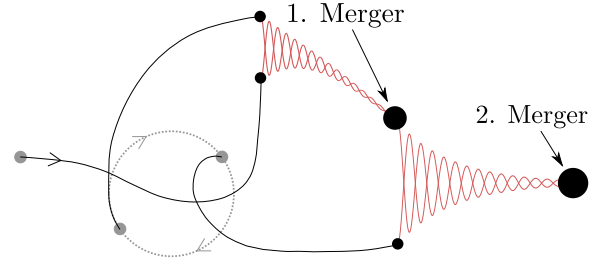


Figure 1. Illustration of a hierarchical merger chain, where two subsequent BBH mergers form from a single three-body interaction. The interaction progresses from left to right, where the BH tracks are highlighted with black thin lines. As seen, the initial configuration is a binary interacting with an incoming single (grey dots). During the interaction, two of three BHs merge, after which the product merges with the remaining single ([Samsing & Ilan 2018b](#)). In this paper we search for such BBH merger pairs.

the mass estimates of the merging BHs, V represents the spatial localization, and t represents the merger times. Subscripts f and s represent the first and second merger, respectively. We do not use the spins of the BHs due to large uncertainties in the spin measurements (e.g. [Abbott et al. 2019a](#)); however, we do hope this becomes possible later, as spin adds an additional strong constraint (the BH formed in the first merger typically appears in the second merger with a spin of ~ 0.7 (e.g. [Berti et al. 2007](#); [Fishbach et al. 2017](#))).

For writing down the likelihoods we assume that the individual BH masses in the first merger follow a power law distribution with index -2.35 between $5-50M_\odot$ (denoted as \mathcal{M}_i) ([Abbott et al. 2016](#)). We further assume 5% of the total initial BH mass is radiated during merger, as suggested by previous detections and theory (e.g. [Abbott et al. 2019a](#)). Hence, for BHs which are a result of a previous merger the corresponding mass spectrum is the self-convolution of the \mathcal{M}_i mass spectrum (denoted as \mathcal{M}_c) with its values reduced by 5%. We marginalize over these mass distributions and a r^2 distribution for distance (r) when calculating the likelihoods. We are well aware that different dynamical channels predict different BH mass distributions; however, we do find that our results do not strongly depend on the chosen model. The power of the search mainly comes from comparing two detections with each other rather than comparing them to a prior distribution. The full expression for the likelihood ratio is given in the Appendix.

2.2 Generating the background distribution

Our significance test is based on a frequentist p-value assignment via comparison with a background distribution. In order to have the background distribution, we perform BBH merger simulations and localize them with BAYESTAR ([Singer & Price 2016](#); [Singer et al. 2016](#)). The simulations assume that the mass of BHs that are not a result of a previous merger is drawn independently from our assumed initial BH mass distribution \mathcal{M}_i . The mergers are distributed uniformly in comoving volume, and the orientation of their orbital axes are uniformly randomized. We assume the BH spins to be aligned with the orbital axis and we don’t include precession ([Corley et al. 2019](#)). We use the reduced-order-model (ROM) SEOBNRv4 waveforms ([Bohé et al. 2017](#)), and the cosmological parameters from the nine-year WMAP observations ([Hinshaw et al. 2013](#)). The simulated detection pairs are made at O2 sensitivity for different detector combinations corresponding to first and second merger detected by either the LIGO Hanford-LIGO Livingston (HL) combination or the LIGO Hanford-LIGO Livingston-Virgo (HLV)

combination. We denote the pairs that are both detected by HL as HL-HL, both by HLV as HLV-HLV, first by HL and second by HLV as HL-HLV, and first by HLV and second by HL as HLV-HL.

In order to construct the background distributions for the likelihood ratios, we need the same inputs as real detections. For this, we first assume that there is 5% mass loss in the merger to have a central value for the final mass. Second, in order to include realistic detection uncertainties, we broaden the exact masses to triangular distributions whose variances depend on the signal-to-noise ratio (SNR) of the detections and the distributions' modes are the exact masses. We use the triangular distributions for imitating the asymmetry of the estimates in the real detections around the median (Abbott et al. 2019a). For determining the upper and lower bounds of the triangular likelihood distributions of masses we use a linear fit whose parameters are obtained by fitting a line to the relative 90% confidence intervals of the mass estimate likelihoods of real detections (which is obtained by dividing the posterior distribution to prior distribution from the parameter estimation samples) as a function of detection SNR. This fit is done separately for both component masses and the final masses. The minimum relative uncertainty is bounded at 5% which is the lowest uncertainty from real detections (Abbott et al. 2019a).

Before moving on the results of our search, in order to estimate the possible capability of our search, we created artificial triple merger pairs by drawing the initial BH masses from the \mathcal{M}_i spectrum and distributing the pairs uniformly in comoving volume. For the best case scenario, HLV-HLV detection, we found that $\sim 90\%$ of the merger pairs have more than one sided 3σ ($p\text{-value} \leq 1/740$) significance. For the HLV-HL, HL-HLV and HL-HL scenarios, the ratios of the pairs that have more than 3σ significance to the total number of pairs are $\sim 70\%$, 60% and 20% respectively. This shows the importance of having better localization with the 3rd detector for this analysis.

3 RESULTS AND DISCUSSION

In this section we show and discuss our results for the 18 BBH mergers. We use both the samples for the 10 GWTC-1 and 18 IAS-Princeton mergers and find p-values for each separately. These merger counts give us a total of 45 possible hierarchical merger pair combinations for GWTC-1 and 153 for the IAS-Princeton sample.

3.1 Event Pair Significance

In Fig. 2 we show the 2 most significant event pairs from our search. The most significant merger pair GW151012 (first merger) and GW170809 (second merger) has an individual p-value of 2.5% from the GWTC-1 sample, meaning that only 2.5% of the background event pairs are more significant than this. Its p-value from the IAS-Princeton sample is 4.8%, slightly higher. The significance of the pair comes from the matching of the primary mass of GW170809 with the mass of the final black hole of GW151012. However the primary mass of GW170809 ($\sim 35M_\odot$) is well below the (hypothesized) pair-instability mass limit and GW170809 was not thought of a potential hierarchical merger result.

Our second most significant event involves GW170729 (first merger) and GW170817A (second merger), with individual p-value of 3.1%. GW170817A's primary mass exceeds the (hypothesized) pair-instability mass limit (its median is $\sim 50M_\odot$ with support up to $\sim 80M_\odot$) suggesting it could be the result of a previous merger (Gayathri et al. 2020). Our analysis suggests that GW170729 is

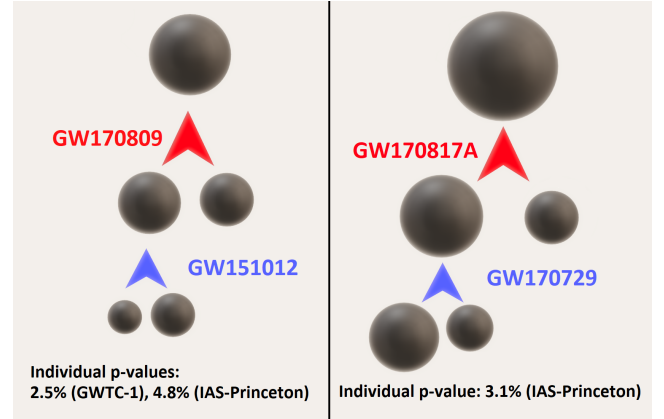


Figure 2. The consecutive merger scenarios for the two most significant event pairs with their individual p-values for IAS-Princeton and GWTC-1 samples. The second pair is only present in the IAS sample since GW170817A is not listed in GWTC-1.

a plausible previous merger for GW170817A in the hierarchical merger scenario, through the GW170817A's primary black hole, as in the GW170809-GW151012 pair. However, as explained at the end of the section, after one accounts for the multiple hypothesis testing correction, none of the event pairs analysed can be considered significant enough for a decisive discovery.

GW170729, itself also has a primary mass estimation similar to GW170817A's primary mass which indicates it may also be result of a previous merger (Abbott et al. 2019a; Yang et al. 2019a)(cf. Kimball et al. 2020). However, the significance of event pairs involving GW170729 as the second merger in our analysis are lower; the two most significant pairs being GW170729-GW151012 and GW170729-GW170403. The individual p-values are 5.5% (GWTC-1) and 17% (IAS-Princeton) for GW170729-GW151012, and 11% (IAS-Princeton) for GW170729-GW170403.

Finally, we notify that as the number of events increases, we will inevitably have low p-value event pairs. To account for this, one has to include a 'multiple hypothesis correction', which in our case brings a factor of 198 (the number of analysed merger pairs) to the individual p-values. After this correction, none of the event pairs can be considered significant. When we compare the significance of GW170809-GW151012 pair with our artificially generated triple pairs detected with HL-HLV combination, we find that $\sim 98\%$ of artificially generated pairs to be more significant than the GW170809-GW151012 pair. Similarly for the GW170817A-GW170729 pair, $\sim 99\%$ of the artificially generated HLV-HLV pairs are more significant.

3.2 Limits on hierarchical triple merger rates

We start by estimating the upper limits on the rate density of hierarchical merger pairs given the absence of an observed pair during O1 and O2. For this we assume that the first mergers in the hierarchical chain scenario are Poisson point processes with a uniform rate density per comoving volume, R , and that the temporal difference between the two mergers, t_{12} , follows a power law distribution $P(t_{12} < T) \propto (T/t_{\max})^\alpha$, where t_{\max} ($T \leq t_{\max}$) and α ($\alpha > 0$) are parameters that are linked to the underlying dynamical process (e.g. Samsing & Ilan 2018b). We further assume the duty cycle of each given time period is the same during the observing runs, i.e., we do not consider the non-uniformity of running times during

the runs. The duty cycle for having at least two operating detectors during O1 is 42.8% and during O2 is 46.4% (Vallisneri et al. 2015; Abbott et al. 2019a). Studies have shown that about half of all BBH mergers forming during three-body interactions will appear with an eccentricity $e > 0.1$ at 10 Hz (Samsing et al. 2020; Rodriguez et al. 2018a). However, current matched filter search template banks only include circular orbits (Abbott et al. 2019c) (except a recent study on binary neutron star mergers (Nitz et al. 2020)). Non-template based searches are able to recover eccentric binaries (Abbott et al. 2019b), but with somewhat lower sensitivity compared to that of template based searches for circular binaries for the masses considered here. Hence, for simplicity, we consider a 50% loss of efficiency as well. Together with this loss, we denote the overall duty cycles as κ_1 and κ_2 , respectively for O1 and O2, and the O1 duration by Δt_1 , the O2 duration by Δt_2 , and the time in between O1 and O2 by Δt_0 (O1 lasted about 4 months, O2 lasted about 9 months and they had about 10 months in between). The search comoving volumes are denoted for O1 and O2 by C_1 and C_2 , respectively. These two volumes, C_1 and C_2 , we estimate by (i) using the ratios of the ranges of the LIGO instruments in the O1, O2 and O3 runs; (ii) the search comoving volume for the O3 run in Abbott et al. (2020); (iii) neglecting the contribution to the search comoving volume in O3 by Virgo (due to having less than the half range of LIGO detectors), and (iv) assuming independent 70% duty cycles for the LIGO detectors in O3 (Abbott et al. 2020). We estimate C_1 to be $0.07 \text{ Gpc}^3 \text{ year/year}$ and C_2 to be $0.14 \text{ Gpc}^3 \text{ year/year}$. Following this model we then calculate the probability \mathcal{P} of not seeing a hierarchical merger pair during O1 and O2 (The full expression for \mathcal{P} is found in the Appendix). Results are presented in Fig. 3, which shows the frequentist 90% upper limit for the rate density R that satisfies $\mathcal{P} = 0.1$, for different values of t_{\max} and α . We have chosen t_{\max} values between 10 and 10^7 years which are the expected order magnitudes for prompt mergers and non-prompt mergers (see Samsing & Ilan (2018b)). Hence, those represent the limiting cases of all mergers being prompt and non-prompt. As seen, the upper rate density varies between $\sim 150 - 210 \text{ year}^{-1} \text{ Gpc}^{-3}$ for our chosen range of values.

We now investigate the expected future limits for triple hierarchical mergers assuming a null result when the third observing run of LIGO and Virgo (O3), and planned fourth observing run (O4) with KAGRA (Aso et al. 2013), also are included in our search. O3 started on April 1st, 2019, and is planned to have 12 months of observing duration, with a one month break in October 2019. Although O4 dates remain fluid, it is estimated to be in between 2021/2022-2022/2023 (Abbott et al. 2020). For our study we assume O3 and O4 to last for a year, with O4 starting in January 2022. The comoving search volumes in O3 and O4 are estimated to be $0.34 \text{ Gpc}^3 \text{ year/year}$ and $1.5 \text{ Gpc}^3 \text{ year/year}$, respectively. Although it will be more accurate to include the contribution from Virgo to these volumes, we here neglect its contribution to the duty cycles in a conservative manner and assume 70% independent duty cycles for the LIGO detectors (Abbott et al. 2020). We adopt the median expected BBH merger detection counts from Abbott et al. (2020), which are 17 and 79 for O3 and O4 respectively. Our derived lowest limits with the inclusion of O3 and O4 is shown in Fig. 3. As seen, the rate densities are now $\sim 11 - 110 \text{ year}^{-1} \text{ Gpc}^{-3}$.

We end our analysis by investigating the upper limits for the fractional contribution from the first mergers of the hierarchical triple mergers to the total BBH merger rate. For the detection number and duration of the O1 and O2 runs, then at 90% confidence, the upper limits of the fractional contribution for the model parameters we consider in Fig. 3 are all ≈ 1 . We get more informative upper limits when we consider absence of merger pairs in the O3 and O4

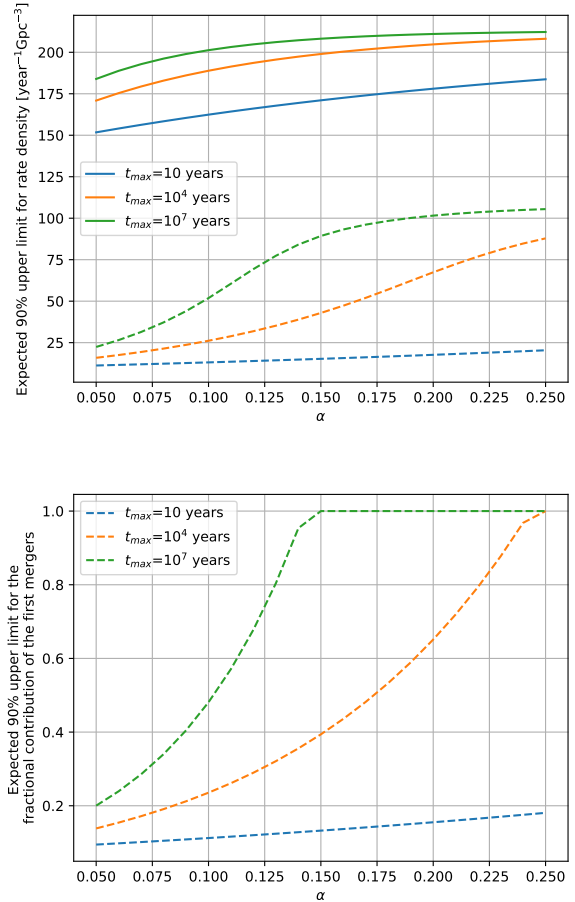


Figure 3. Expected 90% upper limit of density (top) and fractional contribution to the total observed BBH merger rate (bottom) for the first mergers of the triple hierarchical mergers. *Solid* lines show the rate densities considering the absence of a significant event pair in O1 and O2 runs. *Dashed* lines show the rate densities assuming the absence of a significant event pair when O3 and O4 are also included.

runs as illustrated in the lower panel of Fig. 3. As seen, the upper limits now vary between $\sim 0.1 - 1$.

Finally, we stress that our rate estimates from this section are associated with large uncertainties, mainly due to unknowns in the underlying dynamical model. For example, the functional shape of our adopted $P(t_{12} < T)$ -model from Section 3.2, depends in general on both the BH mass hierarchy, the exact underlying dynamics, the initial mass function, as well as on the individual spins of the BHs (e.g. Samsing & Ilan 2018b); all of which are unknown components. Another aspect is how the rate limit depends on other measurable parameters, such as orbital eccentricity and BH spin. For example, in Samsing & Ilan (2018b) it was argued that most hierarchical three-body merger chains are associated with high eccentricity; a search for eccentric BBH mergers, as the one performed in Romero-Shaw et al. (2019), can therefore be used to put tight constraints on this scenario. Another example, is the effective spin parameter, χ_{eff} , which was used to argue that the primary BH of GW170729 is likely not a result of a previous BBH merger despite its relative high mass and spin (Kimball et al. 2020). However, we are actively working on improving our search algorithm both through the inclusion of

eccentricity and spin. Having a fast and accurate pipeline searching for correlated events might also be useful for putting constraints on gravitationally lensed events.

4 CONCLUSION

We presented a search method (Section 2) for detecting hierarchical GW merger pair events resulting from binary-single interactions (see Fig. 1), and applied it to the public available O1/O2 data from the LIGO and Virgo collaborations. Using a frequentist p-value assignment statistics we do not find any significant GW merger candidates in the data that originate from a hierarchical binary-single merger chain (Section 3.1). Using a simple model for describing the time between the first and second merger (Section 3.2), we estimated the upper limit on the rate of hierarchical mergers from binary-single interactions from the O1/O2 runs to be $\sim 150 - 210 \text{ year}^{-1} \text{ Gpc}^{-3}$ for varying parameter values of our time-difference model. Assuming no significant merger pairs in the O3/O4 runs we find the upper limit reduces to $\sim 11 - 110 \text{ year}^{-1} \text{ Gpc}^{-3}$, corresponding to a rate that relative to the total merger rate is $\sim 0.1 - 1.0$. The theoretical predicted rate of hierarchical GW merger pair events is highly uncertain; however, we have argued and shown that both a detection and a non-detection of merger pairs can provide useful constraints on the origin of BBH mergers. In future work we plan on including both eccentricity and BH spin parameters in our search for hierarchical GW merger pair events. Moreover, considering the expectancy of such events happening in dense environments, known AGNs or other plausibly related dense environments can also be used to correlate with the spatial reconstruction of the events in the search.

ACKNOWLEDGMENTS

The authors are grateful for the useful feedback of Christopher Berry and Jolien Creighton. The authors thank the University of Florida and Columbia University in the City of New York for their generous support. The Columbia Experimental Gravity group is grateful for the generous support of the National Science Foundation under grant PHY-1708028. D.V. is grateful to the Ph.D. grant of the Fulbright foreign student program. A.S. is grateful for the support of the Columbia College Science Research Fellows program. J.S. acknowledges support from the European Unions Horizon 2020 research and innovation programme under the Marie Skłodowska-Curie grant agreement No. 844629. The authors are grateful to Leo Singer of GSFC for the BAYESTAR package and his valuable help with our use case scenario. This research has made use of data, software and/or web tools obtained from the Gravitational Wave Open Science Center (<https://www.gw-openscience.org>), a service of LIGO Laboratory, the LIGO Scientific Collaboration and the Virgo Collaboration. LIGO is funded by the U.S. National Science Foundation. Virgo is funded by the French Centre National de Recherche Scientifique (CNRS), the Italian Istituto Nazionale della Fisica Nucleare (INFN) and the Dutch Nikhef, with contributions by Polish and Hungarian institutes.

DATA AVAILABILITY

The data underlying this article were accessed from <http://dx.doi.org/10.7935/KSX7-QQ51> and <https://github.com/>

[jroulet/O2_samples](#). The derived data generated in this research will be shared on reasonable request to the corresponding author.

REFERENCES

- Abbott B. P., et al., 2016, *Phys. Rev. X*, 6, 041015
 Abbott B., et al., 2019a, *Physical Review X*, 9, 031040
 Abbott B. P., et al., 2019b, *Phys. Rev. D*, 100, 064064
 Abbott B. P., et al., 2019c, *The Astrophysical Journal*, 883, 149
 Abbott B. P., et al., 2020, Prospects for Observing and Localizing Gravitational-Wave Transients with Advanced LIGO, Advanced Virgo and KAGRA ([arXiv:1304.0670](https://arxiv.org/abs/1304.0670))
 Antonini F., Rasio F. A., 2016, *ApJ*, 831, 187
 Askar A., Szkudlarek M., Gondek-Rosińska D., Giersz M., Bulik T., 2017, *MNRAS*, 464, L36
 Aso Y., Michimura Y., Somiya K., Ando M., Miyakawa O., Sekiguchi T., Tatsumi D., Yamamoto H., 2013, *Phys. Rev. D*, 88, 043007
 Bae Y.-B., Kim C., Lee H. M., 2014, *MNRAS*, 440, 2714
 Banerjee S., Baumgardt H., Kroupa P., 2010, *MNRAS*, 402, 371
 Bartos I., Haiman Z., Marka Z., Metzger B. D., Stone N. C., Marka S., 2017a, *Nature Communications*, 8, 831
 Bartos I., Kocsis B., Haiman Z., Márka S., 2017b, *ApJ*, 835, 165
 Belczynski K., Holz D. E., Bulik T., O’Shaughnessy R., 2016a, *Nature*, 534, 512
 Belczynski K., Repetto S., Holz D. E., O’Shaughnessy R., Bulik T., Berti E., Fryer C., Dominik M., 2016b, *ApJ*, 819, 108
 Berti E., Cardoso V., Gonzalez J. A., Sperhake U., Hannam M., Husa S., Brügmann B., 2007, *Phys. Rev. D*, 76, 064034
 Bird S., Cholis I., Muñoz J. B., Ali-Haïmoud Y., Kamionkowski M., Kovetz E. D., Raccanelli A., Riess A. G., 2016, *Physical Review Letters*, 116, 201301
 Bohé A., et al., 2017, *Phys. Rev. D*, 95, 044028
 Carr B., Kühnel F., Sandstad M., 2016, *Phys. Rev. D*, 94, 083504
 Cholis I., Kovetz E. D., Ali-Haïmoud Y., Bird S., Kamionkowski M., Muñoz J. B., Raccanelli A., 2016, *Phys. Rev. D*, 94, 084013
 Corley K. R., et al., 2019, *MNRAS*, 488, 4459
 D’Orazio D. J., Loeb A., 2018, *Physical Review D*, 97
 De Mink S. E., Mandel I., 2016, *Monthly Notices of the Royal Astronomical Society*, 460, 3545
 Dominik M., Belczynski K., Fryer C., Holz D. E., Berti E., Bulik T., Mandel I., O’Shaughnessy R., 2012, *ApJ*, 759, 52
 Dominik M., Belczynski K., Fryer C., Holz D. E., Berti E., Bulik T., Mandel I., O’Shaughnessy R., 2013, *ApJ*, 779, 72
 Dominik M., et al., 2015, *ApJ*, 806, 263
 Fishbach M., Holz D. E., Farr B., 2017, *ApJ*, 840, L24
 Gayathri V., Bartos I., Haiman Z., Klimentenko S., Kocsis B., Márka S., Yang Y., 2020, *The Astrophysical Journal*, 890, L20
 Hamers A. S., Bar-Or B., Petrovich C., Antonini F., 2018, *ApJ*, 865, 2
 Hinchshaw G., et al., 2013, *ApJS*, 208, 19
 Hoang B.-M., Naoz S., Kocsis B., Rasio F. A., Dosopoulou F., 2018, *The Astrophysical Journal*, 856, 140
 Hong J., Lee H. M., 2015, *MNRAS*, 448, 754
 Janiak A., Bejger M., Charzyński S., Sukova P., 2017, *New Astronomy*, 51, 7–14
 Kimball C., Berry C., Kalogera V., 2020, *Research Notes of the American Astronomical Society*, 4, 2
 LIGO Scientific Collaboration and Virgo Collaboration 2019, Parameter estimation sample release for GWTC-1, [doi:10.7935/KSX7-QQ51](https://doi.org/10.7935/KSX7-QQ51)
 LIGO Scientific Collaboration Virgo Collaboration Abbott B. P., et al., 2019, *Phys. Rev. D*, 100, 104036
 Loeb A., 2016, *ApJ*, 819, L21
 Mandel I., de Mink S. E., 2016, *Monthly Notices of the Royal Astronomical Society*, 458, 2634
 Marchant, Pablo Langer, Norbert Podsiadlowski, Philipp Tauris, Thomas M. Moriya, Takashi J. 2016, *A&A*, 588, A50
 McKernan B., et al., 2018, *ApJ*, 866, 66

- Murguia-Berthier A., MacLeod M., Ramirez-Ruiz E., Antoni A., Macias P., 2017, *ApJ*, **845**, 173
- Neyman J., Pearson E. S., Pearson K., 1933, *Philosophical Transactions of the Royal Society of London. Series A, Containing Papers of a Mathematical or Physical Character*, 231, 289
- Nitz A. H., Capano C., Nielsen A. B., Reyes S., White R., Brown D. A., Krishnan B., 2019, *The Astrophysical Journal*, 872, 195
- Nitz A. H., Lenon A., Brown D. A., 2020, *The Astrophysical Journal*, 890, 1
- O’Leary R. M., Kocsis B., Loeb A., 2009, *MNRAS*, **395**, 2127
- Park D., Kim C., Lee H. M., Bae Y.-B., Belczynski K., 2017, *MNRAS*, **469**, 4665
- Portegies Zwart S. F., McMillan S. L. W., 2000, *ApJ*, **528**, L17
- Rodriguez C. L., Antonini F., 2018, *ApJ*, **863**, 7
- Rodriguez C. L., Morscher M., Pattabiraman B., Chatterjee S., Haster C.-J., Rasio F. A., 2015, *Phys. Rev. Lett.*, **115**, 051101
- Rodriguez C. L., Chatterjee S., Rasio F. A., 2016a, *Phys. Rev. D*, **93**, 084029
- Rodriguez C. L., Haster C.-J., Chatterjee S., Kalogera V., Rasio F. A., 2016b, *ApJ*, **824**, L8
- Rodriguez C. L., Zevin M., Pankow C., Kalogera V., Rasio F. A., 2016c, *ApJ*, **832**, L2
- Rodriguez C. L., Amaro-Seoane P., Chatterjee S., Kremer K., Rasio F. A., Samsing J., Ye C. S., Zevin M., 2018a, *Physical Review D*, 98
- Rodriguez C. L., Amaro-Seoane P., Chatterjee S., Kremer K., Rasio F. A., Samsing J., Ye C. S., Zevin M., 2018b, *Phys. Rev. D*, **98**, 123005
- Romero-Shaw I. M., Lasky P. D., Thrane E., 2019, *MNRAS*, **490**, 5210
- Samsing J., 2018, *Phys. Rev. D*, **97**, 103014
- Samsing J., D’Orazio D. J., 2018, *MNRAS*,
- Samsing J., Ilan T., 2018a, *MNRAS*, **476**, 1548
- Samsing J., Ilan T., 2018b, *Monthly Notices of the Royal Astronomical Society*, 482, 30
- Samsing J., Ramirez-Ruiz E., 2017, *ApJ*, **840**, L14
- Samsing J., MacLeod M., Ramirez-Ruiz E., 2014, *ApJ*, **784**, 71
- Samsing J., MacLeod M., Ramirez-Ruiz E., 2018a, *ApJ*, **853**, 140
- Samsing J., Askar A., Giersz M., 2018b, *ApJ*, **855**, 124
- Samsing J., Venumadhav T., Dai L., Martinez I., Batta A., Lopez M., Ramirez-Ruiz E., Kremer K., 2019a, *Phys. Rev. D*, **100**, 043009
- Samsing J., Hamers A. S., Tyles J. G., 2019b, *Phys. Rev. D*, **100**, 043010
- Samsing J., D’Orazio D. J., Kremer K., Rodriguez C. L., Askar A., 2020, *Physical Review D*, 101
- Sasaki M., Suyama T., Tanaka T., Yokoyama S., 2016, *Physical Review Letters*, **117**, 061101
- Schröder S. L., Batta A., Ramirez-Ruiz E., 2018, *ApJ*, **862**, L3
- Silsbee K., Tremaine S., 2017, *ApJ*, **836**, 39
- Singer L. P., Price L. R., 2016, *Phys. Rev. D*, **93**, 024013
- Singer L. P., et al., 2016, *The Astrophysical Journal*, 829, L15
- Stephan A. P., Naoz S., Ghez A. M., Witzel G., Sitarski B. N., Do T., Kocsis B., 2016, *MNRAS*, **460**, 3494
- Stone N. C., Metzger B. D., Haiman Z., 2017, *MNRAS*, **464**, 946
- Tagawa H., Haiman Z., Kocsis B., 2019, arXiv e-prints, p. arXiv:1912.08218
- Tanikawa A., 2013, *MNRAS*, **435**, 1358
- Vallisneri M., Kanner J., Williams R., Weinstein A., Stephens B., 2015, *Journal of Physics: Conference Series*, 610, 012021
- VanLandingham J. H., Miller M. C., Hamilton D. P., Richardson D. C., 2016, *ApJ*, **828**, 77
- Venumadhav T., Zackay B., Roulet J., Dai L., Zaldarriaga M., 2020, *Physical Review D*, 101
- Woosley S. E., 2016, *ApJ*, **824**, L10
- Yang Y., et al., 2019a, *Phys. Rev. Lett.*, **123**, 181101
- Yang Y., Bartos I., Haiman Z., Kocsis B., Márka Z., Stone N. C., Márka S., 2019b, *ApJ*, **876**, 122
- Zackay B., Dai L., Venumadhav T., Roulet J., Zaldarriaga M., 2019a, Detecting Gravitational Waves With Disparate Detector Responses: Two New Binary Black Hole Mergers (arXiv:1910.09528)
- Zackay B., Venumadhav T., Dai L., Roulet J., Zaldarriaga M., 2019b, *Physical Review D*, 100
- Zevin M., Pankow C., Rodriguez C. L., Sampson L., Chase E., Kalogera V., Rasio F. A., 2017, *ApJ*, **846**, 82
- Zevin M., Samsing J., Rodriguez C., Haster C.-J., Ramirez-Ruiz E., 2019, *ApJ*, **871**, 91

APPENDIX A: LIKELIHOOD RATIO

All BBH mergers are assumed to be uniformly distributed in comoving volume. In this case the likelihood ratio becomes

$$\begin{aligned} \frac{\mathcal{L}(M_f, m_{1,s}, m_{2,s}, V_f, V_s | H_s)}{\mathcal{L}(M_f, m_{1,s}, m_{2,s}, V_f, V_s | H_0)} &= \frac{\int P(M_f, m_{1,s}, m_{2,s} | m', H_s) P(m' | H_s) dm' \int P(V_f, V_s | r, H_s) P(r | H_s) dr d\Omega}{\int P(M_f, m_{1,s}, m_{2,s} | H_0) dm' \int P(V_f, V_s | H_0) dr d\Omega} \\ &= \frac{\int \frac{P(r | V_f) P(r | V_s)}{r^2} dr d\Omega \sum_{\substack{x,y=1,2 \\ x \neq y}} \int \frac{P(m' | M_f)}{P_f(m')} \frac{P(m' | m_{x,s})}{P_{x,s}(m')} \mathcal{M}_c(m') dm' \int \frac{P(m' | m_{y,s})}{P_{y,s}(m')} \mathcal{M}_i(m') dm'}{\int \frac{P(m' | M_f)}{P_f(m')} \mathcal{M}_c(m') dm' \int \frac{P(m' | m_{1,s})}{P_{1,s}(m')} \mathcal{M}_i(m') dm' \int \frac{P(m' | m_{2,s})}{P_{2,s}(m')} \mathcal{M}_i(m') dm'} \quad (A1) \end{aligned}$$

where m' , r and Ω are the integration variables for mass, distance and sky location. $P_f(m')$, $P_{1,s}(m')$ and $P_{2,s}(m')$ are the mass priors used in the parameter estimation. We take these from the parameter estimation sample released in GWTC-1 (LIGO Scientific Collaboration and Virgo Collaboration 2019) and from https://github.com/jroulet/02_samples for the IAS-Princeton sample. The integrals over the spatial localization in the denominator equals unity and are therefore not written. The summed terms in the numerator represent either of the BHs in the second merger resulting from the first merger.

APPENDIX B: PROBABILITY \mathcal{P}

Here we write the probability \mathcal{P} of not seeing a hierarchical merger pair for the parameters R , t_{max} , α , κ_1 , κ_2 , Δt_1 , Δt_2 , Δt_0 , and with the number of seen events, n_i , during O1 ($n_1 = 3$) and O2 ($n_2 = 7$). The condition of not seeing a pair of hierarchical mergers is to see at most one of the mergers in the pair.

$$\begin{aligned} \mathcal{P} &= \left[\sum_{i=0}^{n_1} \text{Poisson}(i, \kappa_1 R \Delta t_1 C_1) \frac{i!}{\Delta t_1^i} \int_0^{\Delta t_1} \int_0^{\tau_i} \dots \int_0^{\tau_2} \left[1 - \kappa_2 \left(\frac{\Delta t_1 + \Delta t_2 + \Delta t_0 - \tau_1}{t_{max}} \right)^\alpha + \kappa_2 \left(\frac{\Delta t_1 + \Delta t_0 - \tau_1}{t_{max}} \right)^\alpha - \kappa_1 \left(\frac{\Delta t_1 - \tau_1}{t_{max}} \right)^\alpha \right] \times \right. \\ &\dots \times \left[1 - \kappa_2 \left(\frac{\Delta t_1 + \Delta t_2 + \Delta t_0 - \tau_{i-1}}{t_{max}} \right)^\alpha + \kappa_2 \left(\frac{\Delta t_1 + \Delta t_0 - \tau_{i-1}}{t_{max}} \right)^\alpha - \kappa_1 \left(\frac{\Delta t_1 - \tau_{i-1}}{t_{max}} \right)^\alpha \right] \\ &\times \left[1 - \kappa_2 \left(\frac{\Delta t_1 + \Delta t_2 + \Delta t_0 - \tau_i}{t_{max}} \right)^\alpha + \kappa_2 \left(\frac{\Delta t_1 + \Delta t_0 - \tau_i}{t_{max}} \right)^\alpha - \kappa_1 \left(\frac{\Delta t_1 - \tau_i}{t_{max}} \right)^\alpha \right] d\tau_1 \dots d\tau_{i-1} d\tau_i \Big] \\ &\times \left[\sum_{i=0}^{n_2} \text{Poisson}(i, \kappa_2 R \Delta t_2 C_2) \frac{i!}{\Delta t_2^i} \int_0^{\Delta t_2} \int_0^{\tau_i} \dots \int_0^{\tau_2} \left[1 - \kappa_2 \left(\frac{\Delta t_2 - \tau_1}{t_{max}} \right)^\alpha \right] \times \dots \times \left[1 - \kappa_2 \left(\frac{\Delta t_2 - \tau_{i-1}}{t_{max}} \right)^\alpha \right] \times \left[1 - \kappa_2 \left(\frac{\Delta t_2 - \tau_i}{t_{max}} \right)^\alpha \right] d\tau_1 \dots d\tau_{i-1} d\tau_i \right] \quad (B1) \end{aligned}$$

with $\text{Poisson}(n, k)$ being the probability of seeing n events from the Poisson point process with mean k . $\frac{i!}{\Delta t}$ is the value of joint probability distribution of Poisson arrival times given that there are i events in time interval Δt . The integrals give the probability of not seeing any of the second mergers of i observed first mergers during the observation times. The first term in Eq. (B1) gives the probability of not seeing an hierarchical merger pair whose first event can happen during O1 and second event can happen during O1 or O2. The second term gives the probability of not seeing an hierarchical merger pair whose both mergers can happen during O2. Multiplication of them gives us the probability of not seeing an hierarchical pair during O1 and O2. We use the integral identity

$$\int_0^a \int_0^{\tau_i} \dots \int_0^{\tau_2} f(\tau_1) \times \dots \times f(\tau_{i-1}) \times f(\tau_i) d\tau_1 \dots d\tau_{i-1} d\tau_i = \left(\int_0^a f(\tau_1) d\tau_1 \right)^i \frac{1}{i!} \quad (B2)$$

to simplify the expression for \mathcal{P} .

$$\begin{aligned} \mathcal{P} &= \left[\sum_{i=0}^{n_1} \text{Poisson}(i, \kappa_1 R \Delta t_1 C_1) \frac{1}{\Delta t_1^i} \left[\int_0^{\Delta t_1} \left[1 - \kappa_2 \left(\frac{\Delta t_1 + \Delta t_2 + \Delta t_0 - \tau_1}{t_{max}} \right)^\alpha + \kappa_2 \left(\frac{\Delta t_1 + \Delta t_0 - \tau_1}{t_{max}} \right)^\alpha - \kappa_1 \left(\frac{\Delta t_1 - \tau_1}{t_{max}} \right)^\alpha \right] d\tau_1 \right]^i \right] \\ &\times \left[\sum_{i=0}^{n_2} \text{Poisson}(i, \kappa_2 R \Delta t_2 C_2) \frac{1}{\Delta t_2^i} \left[\int_0^{\Delta t_2} \left[1 - \kappa_2 \left(\frac{\Delta t_2 - \tau_1}{t_{max}} \right)^\alpha \right] d\tau_1 \right]^i \right] \quad (B3) \end{aligned}$$